

## COBEM-2017-1446

### STUDY OF SOLAR CHIMNEY WITH OPENFOAM

Lucía Romeo  
Pedro Galione  
Pedro Curto

Instituto de Ingeniería Mecánica y Producción industrial - Facultad de Ingeniería - Universidad de la República  
lromeo@fing.edu.uy  
pgalione@fing.edu.uy  
pcurto@fing.edu.uy

**Abstract.** The aim of this work is to study the thermodynamic phenomena and performance of solar chimneys using OpenFOAM. OpenFOAM is an open-source computational fluid dynamics software used by a wide international community. Although several different models for simulating the flow and heat transfer in fluids, heat transfer in solid media and also radiation heat exchange are available, not all the combinations of the individual models are already available, in the down loadable distribution, to be used in the same problem. In this work, mass, momentum, energy and radiation exchange between surfaces equations in OpenFOAM are combined for developing solar chimney simulations. A case of a solar dryer is used to test the performance of the obtained model and the results obtained are compared against numerical and experimental data obtained from the literature.

**Keywords:** solar chimney, OpenFOAM, radiation, convection, conduction.

#### 1. INTRODUCTION

In the last decades the fast development of global economy, population increase and living standards have imposed an increasing pressure on natural resources, making a matter of importance the study of renewable energy sources. The combustion of fossil fuels to generate electric energy has significantly contributed to global warming by releasing greenhouse gases which have been found to produce significant negative environmental effects (Zhou *et al.*, 2012).

For these reasons renewable and sustainable energy sources are nowadays considered to be a key element for sustainable development of the worldwide economy. The Solar Updraft Power Plant (or Solar Chimney) technology addresses the idea of combining both kinds of renewable energy: wind and solar (Lupi *et al.*, 2004).

The focus of this work is to be able to perform detailed numerical analysis of solar chimneys. This technology consists of a collector, where the air is heated by the incidence of solar radiation, and the chimney, which imposes a pressure gradient that favors air circulation. Depending on its application, this system may include a turbine (with electric power generating purposes) or not (e.g. performing as a dryer). A schematic representation of the system can be seen in "Fig. 1".

Numerical simulations are performed using the OpenFOAM free software to solve the equations of thermo-convective phenomena, soil heat conduction and radiation exchange between surfaces.

#### 2. NUMERICAL MODEL

Navier-Stokes equations, radiation heat exchange between surfaces and heat flux to the ground are solved using OpenFOAM. Air and ground domains are combined using the available multi-region tools.

A combination between buoyantBoussinesqPimpleFoam and chtMultiRegionFoam solvers was implemented, to solve multi-region cases using Boussinesq approximation in the fluid zones. Also, radiation balance was added to the solver, considering sky, sun and surfaces contributions.

For the motion and heat transfer in the air, RAS (Reynolds-averaged simulation) standard k-epsilon turbulence model for incompressible fluid with the Boussinesq approximation has been used.

The solved equations used are:

**Continuity:**

$$\frac{\partial \bar{u}_j}{\partial x_j} = 0 \quad (1)$$

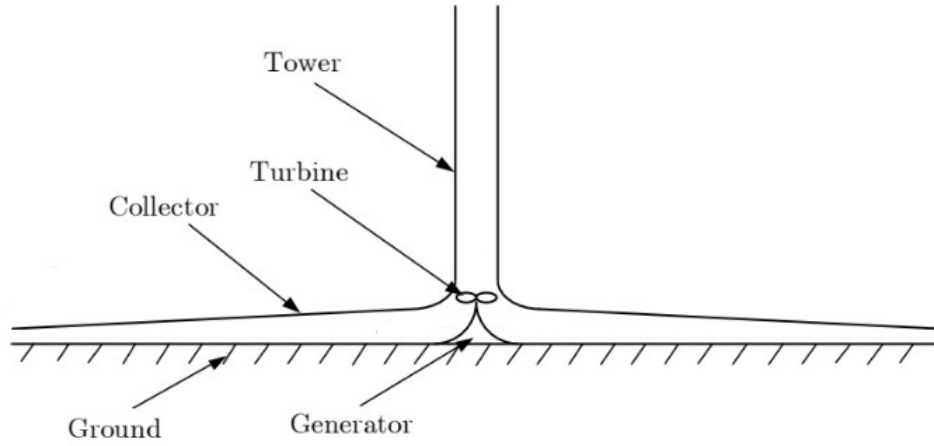


Figure 1. Schematic solar chimney power plant. Extracted from Pretorius (2004)

**Momentum:**

$$\frac{\partial \bar{u}_i}{\partial t} + \frac{\partial (\bar{u}_j \bar{u}_i)}{\bar{x}_i} - \frac{\partial}{\partial x_j} \left( \nu_{eff} \left[ \left( \frac{\partial \bar{u}_i}{\partial x_j} + \frac{\partial \bar{u}_j}{\partial x_i} \right) - \frac{2}{3} \left( \frac{\partial \bar{u}_k}{\partial x_k} \right) \delta_{ij} \right] \right) = \frac{-\partial \tilde{p}}{\partial x_i} + g_i (1 - \beta (\bar{T} - T_0)) \quad (2)$$

where  $\nu_{eff}$  is the effective kinematic viscosity, considering the turbulent contribution.

**Energy:**

$$\frac{\partial \bar{T}}{\partial t} + \frac{\partial}{\partial x_j} (\bar{T} \bar{u}_j) - \frac{\partial}{\partial x_k} \left( k_{eff} \frac{\partial \bar{T}}{\partial x_k} \right) = 0 \quad (3)$$

where  $k_{eff}$  is a combined heat transfer coefficient, as explained in “Openfoamwiki (2014)”.

Furthermore, the thermal interaction between ground, inner air, cover and outer air is solved by considering convection and radiation heat exchange between surfaces and heat conduction within the ground (shown in “Fig. 2”). Their equations are written below.

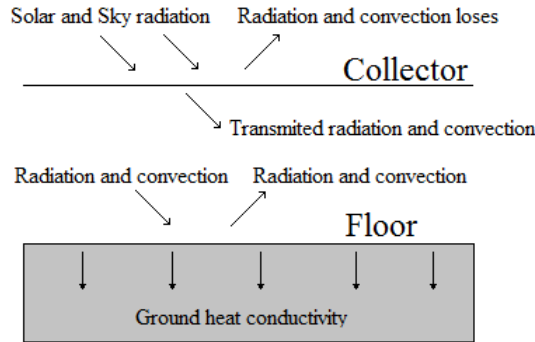


Figure 2. Schematics of heat transfer in the collector zone

To simplify the case of study,  $T_{coll}$  and  $T_{floor}$  were taken uniform among the entire surfaces, imposing that every face-cell which belongs to the patch in matter (collector and floor respectively) has the same calculated temperature.

The following parameters, calculated in “Eq. (4)” and “Eq. (5)”, are necessary to write collector and floor energy balance equations:

$$h_{rad} = \frac{\sigma (T_{floor}^2 + T_{coll}^2) (T_{floor} + T_{coll})}{\frac{1-\epsilon_{floor}}{\epsilon_{floor}} + \frac{1-\epsilon_{coll}}{\epsilon_{coll}} + 1} \quad (4)$$

$$h_{rad_{sky}} = \epsilon_{coll} \sigma (T_{coll}^2 + T_{sky}^2) (T_{coll} + T_{sky}) \quad (5)$$

**Collector:**

$$\alpha_{coll}G_{sun}A_{coll} + h_{rad}A_{coll}(T_{floor} - T_{coll}) = k_{air} \left[ T_{coll} \sum_i^n \frac{A_{coll_i}}{d_{np_i}} - \sum_i^n \frac{T_c A_{coll_i}}{d_{np_i}} \right] + h_{rad_{sky}}(T_{coll} - T_{sky})A_{coll} \quad (6)$$

**Floor:**

$$(\alpha_{floor}\tau_{coll})G_{sun}A_{floor} + h_{rad}A_{floor}(T_{coll} - T_{floor}) = k_{air}T_{floor} \sum_i^n \frac{A_{floor_i}}{d_{np_i}} - k_{air} \sum_i^n \frac{T_c A_{floor_i}}{d_{np_i}} + k_{soil}T_{floor} \sum_i^n \frac{A_{floor_i}}{d_{np_i}} - k_{soil} \sum_i^n \frac{T_c A_{floor_i}}{d_{np_i}} \quad (7)$$

**Energy balance within the ground:**

$$\frac{\partial \bar{T}}{\partial t} - \frac{\partial}{\partial x_k} \left( k_{eff} \frac{\partial \bar{T}}{\partial x_k} \right) = 0 \quad (8)$$

where a fixed temperature has been used as boundary condition at certain depth.

Parameters used:  $\alpha_{coll}$  and  $\alpha_{floor}$  are collector and floor absorptivity when surfaces are irradiated by the sun (short wavelength),  $G_{sun}$  is the total sun irradiation that reaches the surfaces (measured in  $W/m^2$ ),  $A_{coll}$  and  $A_{floor}$  are collector and floor surfaces,  $d_{np_i}$  are the distances between cell and patch face centers (considering only those cells neighboring the patches),  $T_c$  represent cell temperature,  $k_{air}$  and  $k_{soil}$  are air and soil thermal conductivities.

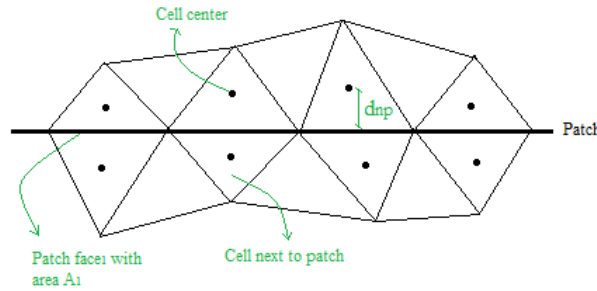


Figure 3. Parameters form mesh used un the equations

$h_{rad}$  and  $h_{rad_{sky}}$  are radiation coefficients, the first one taking into account the exchange between surfaces (emitting in the long wavelength spectrum, infrared radiation) and the second one regarding sky and collector interaction. In this model, the sky was considered as a black body with uniform temperature, with emissivity equal to unity. In “Eq. (4)” and “Eq. (5)”  $\sigma$  is the Stefan-Boltzmann constant,  $\epsilon_{floor}$  and  $\epsilon_{coll}$  are surface emissivities.

Once “Eq. (6)” and “Eq. (7)” are solved, the resulting temperatures are used to calculate the total radiation heat that reaches both surfaces. These values were later imposed to the OpenFOAM boundary condition.

An experimental case of a solar dryer, obtained from “Maia *et al.* (2009)” is used for validating the model.

**3. CASE SETTINGS**

As it can be seen in “Fig. 3” an unstructured mesh was used. It was made as a wedge with only one cell in  $z$  direction, so 2D simulations can be carried out. Axi-symmetry around the chimney axis was considered. Wall boundary condition was used for chimney, collector and floor. In top and lateral borders of the domain, some kind of inlet-outlet conditions are imposed.

Several cases were carried out in the search for the appropriate boundary conditions, because the convergence depends on their selection and the refinement of the mesh. For collector and floor patches, turbulentTemperatureRadCoupled-Mixed OpenFOAM temperature boundary condition was adopted. This boundary condition takes as an input parameter the radiation heat calculated by the method explained in previous section, performing an energy balance to the surface considering convection and conduction terms when present.

As shown in “Fig. 4”, for multi-region cases, the mesh is divided into three regions: air (containing the tower system); and ground, which is divided in two regions, one below the collector and the other one beyond. Both regions are connected through a border condition imposing equal temperature and heat flux.

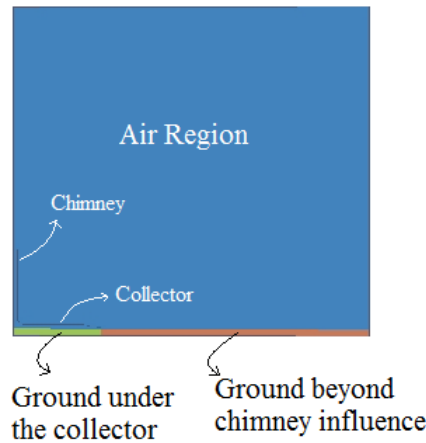


Figure 4. Mesh regions

#### 4. RESULTS AND DISCUSSIONS

Results of velocity and temperature fields inside the chimney and the collector were obtained.

##### 4.1 Multi-region case

In this case a solar radiation value of  $480W/m^2$  (Maia *et al.*, 2009) was imposed and the solver was run until the condition of stationary state is reached inside the tower. Volumetric flow, average temperatures and velocities are calculated at different heights of the chimney and different radius of the collector to verify mass conservation and see if results are coherent with temperature variation. The ambient temperature used for simulation was  $290K$  and  $T_{sky}$  was  $263K$ .

The purpose of the following image, “Fig. 5”, is to show that after  $650s$  approximately, the steady state condition for the flow inside the tower is reached. The fact that temperature starts to rise just around  $270s$  is due to the fact that the final radiation value was introduced to the program as a ramp function of time, to avoid abrupt changes in temperature values and therefore problems with simulation calculation.

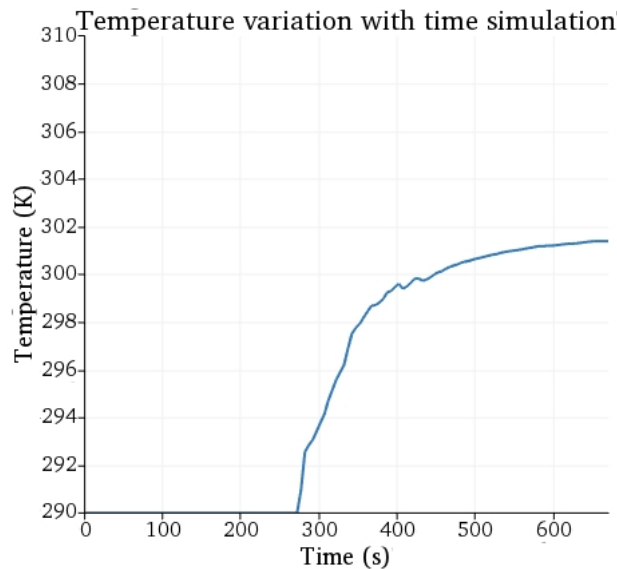


Figure 5. Temperature inside chimney region

In “Tab. 1” results for velocity and temperature were taken at different heights along the chimney. As the chimney section is constant, they all have the same area (with a value of  $0,00436m^2$ ). Exp.  $U$  and Exp.  $\Delta T$  represent average experimental values obtained inside the tower (Maia *et al.*, 2009). These results show that solution reached by OpenFOAM satisfactorily approaches the expected values (when modeling air region with the established parameters). The variation between velocity values may be due to numerical errors. “Table 2” shows results obtained with OpenFOAM for different radius under the cover. Velocities in the collector zone were very low, making it difficult to physically measure them, so there are no values to corroborate them.

Table 1. Results inside the chimney for different heights, with  $\Delta T = T_{flow} - T_{ambient}$ .

Ht(m)	$\Delta T$	Average U (m/s)	Volumetric flow ( $m^3/s$ )	Exp. U (m/s)	Exp. $\Delta T$
2.46	7.47	2.24	0.00979	2.2 ± 0.2	4.0 ± 2.0
3.69	7.32	2.24	0.00979		
4.92	7.35	2.23	0.00975		
6.15	7.36	2.27	0.00992		
9.22	7.29	2.16	0.00943		
11.07	7.36	2.31	0.01007		

Table 2. Results inside the collector for different radius, with  $\Delta T = T_{flow} - T_{ambient}$ .

Rc(m)	Average T (K)	$\Delta T$	Average U (m/s)	Area ( $m^2$ )	Volumetric flow ( $m^3/s$ )
1.87	297.2	7.25	0.302	0.03273	0.00989
5.63	296.5	6.50	0.099	0.0981	0.00978
11.25	293.3	3.33	0.089	0.1079	0.00964

The ground under the collector is modeled with bi-dimensional heat conduction, using the same boundary condition as for the cover on floor surface, taking into account the energy balance to update its temperature. A constant temperature of  $290K$  was considered at  $1m$  depth. Time simulation to calculate soil temperature distribution is considerable high when starting from uniform temperature condition. For that reason initial temperature gradient is set in this region.

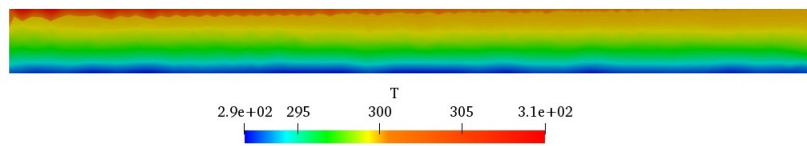


Figure 6. Soil temperature distribution

Table 3. Soil temperature distribution.

Depth(m)	Average T (K)	Exp. T (K)
-0.15	299.8	301
-0.30	299.4	303
-0.40	299.0	305

“Table 3” shows that there are still differences with the experimental data from “Maia *et al.* (2009)”, due to not having adopted the exact same initial distribution and not being able to simulate several days in an acceptable time. It is worth mentioning that the experimental temperature distribution shows increasing temperatures with depth, which means that in previous times heat was being stored. At the moment when experimental data was registered, heat was being transferred to the surface from the underground, differently from what was occurring in the simulation.

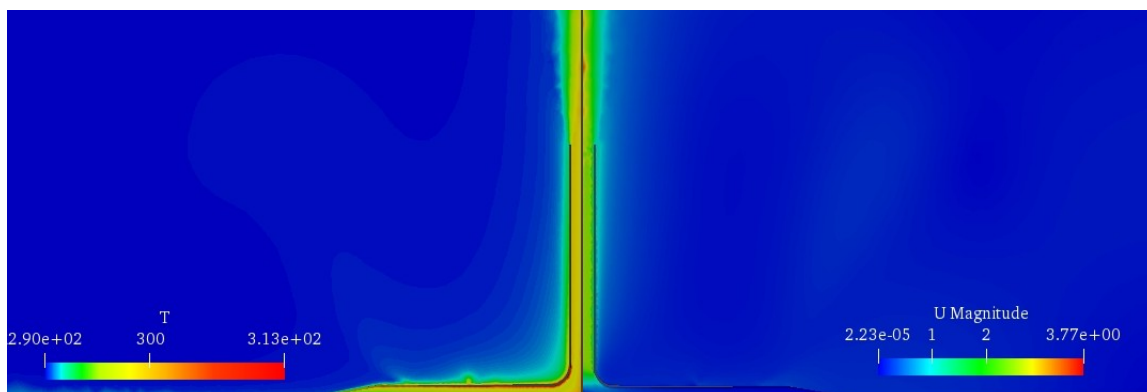


Figure 7. Temperature and velocity field

“Figure 7” shows temperature and velocity fields for the test case. An interesting result obtained, which can only be detected if the outer air of the system is simulated, is that the highest velocity is reached outside the chimney. This may happen due to the fact that the mesh was wedge made (2D), and therefore air flow may be directed towards the chimney joining tower outlet flow, increasing velocity values in the outside. This condition may be different if a 3D mesh is used.

## 5. CONCLUSIONS

A solar chimney model has been developed in the OpenFOAM framework, by the adequate combination of equations of natural convection, radiation heat transfer and heat conduction in the ground, using a multi-region treatment.

It was possible to reach with this model values that are close to reality.

As an interesting result of the test case run, which highlight the importance of simulating the outer air, highest air velocities have been found in the flow outside (over) the chimney.

The developed model allows to simulate air motion and heat transfer within air, ground and their interaction with collector and chimney. With some improvements, detailed performance evaluation can be performed as well as design optimizations. Furthermore, correlations of heat transfer and drag coefficients can be obtained with this model, in order to be used as input into other one-dimensional models intended for long-term evaluations.

## 6. ACKNOWLEDGEMENTS

This work was supported by the Agencia Nacional de Investigación e Innovación (ANII), through the project FSE 2014\_1\_102106.

## 7. REFERENCES

- Lupi, F., Borri, C., Kratzig, W.B. and Niemman, H., 2004. “Solar updraft power plant technology: Basic concepts and structural design”. Encyclopedia of Life Support Systems (EOLSS) (2004). <<https://www.eolss.net/>>.
- Maia, C., Ferreira, A.G., Valle, R.M. and Corte, M., 2009. “Analysis of the airflow in a prototype of a solar chimney dryer”. *Taylor Francis Group, Heat Transfer Engineering*, Vol. 30, pp. 393–399.
- Openfoamwiki, 2014. “BuoyantboussinesqPisoFoam”. <<https://openfoamwiki.net/index.php/BuoyantBoussinesqPisoFoam>>.
- Pretorius, J.P., 2004. *Solar Tower Power Plant Performance Characteristics*. Master’s thesis, University of Stellenbosch.
- Zhou, X., Bernardes, M. and Ochieng, R.M., 2012. “Influence of atmospheric cross flow on solar updraft tower inflow”. *ELSEVIER*, Vol. 42, pp. 393–400.

## 8. RESPONSIBILITY NOTICE

The authors are the only responsible for the printed material included in this paper.